Desalination and Water Treatment
www.deswater.com

doi: 10.1080/19443994.2015.1035343

57 (2016) 8990–9000
April

Taylor & Francis
Taylor & Francis Group

Efficiency of composite permeable reactive barriers for the removal of Cr(VI) from leachates

K. Komnitsas[a,*], G. Bazdanis[a], G. Bartzas[b]

[a]*School of Mineral Resources Engineering, Technical University Crete, 73100 Chania, Greece, Tel. +30 28210 37686; Fax: +30 28210 69554; email: komni@mred.tuc.gr (K. Komnitsas), Tel. +30 28210 37674; email: gbazdanis@gmail.com (G. Bazdanis)*
[b]*School of Mining and Metallurgical Engineering, National Technical University of Athens, 15780 Greece, Tel. +30 210 7722181; email: gbartzas@metal.ntua.gr*

Received 9 January 2015; Accepted 2 March 2015

ABSTRACT

The present paper uses a novel approach and aims to assess the efficiency of composite permeable reactive barriers (PRBs) containing organic material and elemental sulphur for the clean-up of leachates containing Cr(VI) and acetate. The paper also aims to identify the main mechanisms involved in the removal of Cr(VI). Experiments were carried out in laboratory plexiglas columns, with a diameter of 5 cm and length of 50 cm. The feed contained 10 mg L^{-1} Cr(VI) and chemical oxygen demand (0.6 or 6 g L^{-1}). Under the optimum experimental set-up, the PRB exhibited over a period of 270 d excellent Cr(VI) decontamination potential. X-ray diffraction, scanning electron microscopy and energy dispersive spectrometry as well as Fourier transform infrared spectroscopy were used to characterize the exhausted reactive material, identify newly formed mineral phases and elucidate Cr(VI) removal mechanisms. Sorption of the reduced Cr(III) on the organic material as well as precipitation, mainly as $Cr(OH)_3$, are the main Cr(VI) removal mechanisms.

Keywords: Characterization; Cr(VI); Hydrogen sulphide; Mechanisms; Permeable reactive barriers

1. Introduction

Chromium is widely used in a number of industries including steel production, electroplating, galvanizing, leather tanning and wood treatment. Chromium containing effluents, if not properly managed, may contaminate severely soils and water resources [1]. The most common chromium ions present in industrial effluents and wastewaters are Cr(VI) and Cr(III). Cr(VI) is considered as acutely toxic, mutagenic and carcinogenic and thus extremely hazardous to humans and other living organisms, while Cr(III) which at low concentrations is necessary for human nutrition, exhibits low solubility at neutral pH [2,3]. It is underlined that the maximum allowable concentration of chromium in drinking water should not exceed 50 μg L^{-1} [4].

Numerous studies have been carried out for the reduction of Cr(VI) to Cr(III) and thus amelioration of its toxicity in waters/wastewaters and soils. Cr(VI) reduction in industrial effluents may be achieved through chemical or biological means [4–9]. Chemical treatment involves mainly the use of zero-valent iron (ZVI) in various forms [10–13]. Despite the rather high

*Corresponding author.

efficiency of chemical processes, several factors such as the high cost of chemicals and the difficult management of large volumes of the produced sludge should always be considered. Biological reduction of Cr(VI) has been also widely studied [14–20]. The major disadvantage of biological processes is the inhibition of bacterial growth under high chromium concentrations that results in reduced treatment efficiency [21,22]. Final polishing steps may be also required depending on the desired quality of the treated effluent and the disposal or reuse option foreseen [23]. Advanced treatment options, including photo-Fenton and electrocoagulation [24], chelating ion exchange resins [25] or membrane technology [26] may also be considered for the treatment of chromium-containing effluents.

The use of permeable reactive barriers (PRBs) containing ZVI is an established treatment technique for the decontamination of groundwater and contaminated plumes [27–29]. These systems may encounter though, mainly due to iron corrosion and the formation of precipitates, permeability loss and reduced long-term reactivity, thus the efficiency of other alternative inorganic or organic reactive materials has also been investigated. Inorganic reactive materials mainly include limestone, red mud, activated carbon and iron sulphides [30–32]. Organic materials on the other hand, may include agricultural by-products, sewage sludge and other organic wastes [33,34]. Composite PRBs containing mixtures of organic and inorganic reactive materials may prove beneficial in terms of provision of alkalinity and buffering of pH, thus resulting in increased contaminant removal rates by activating more than one clean-up mechanism (e.g. precipitation, co-precipitation and sorption) [35–37]. The most important parameters affecting the efficiency of a PRB include pH, contaminant concentration, flow rate, temperature and retention time. Optimum systems are characterized by limited clogging, increased reactivity, sufficient hydraulic conductivity, environmental compatibility, low cost and long-term stability [38,39].

Hydrogen sulphide which is a reagent characterized by high reduction efficiency and low cost may be considered for the reduction of Cr(VI) in wastewaters and industrial effluents [40,41]. Hydrogen sulphide may be generated through the reduction of elemental sulphur, which is a cheap, non toxic, insoluble in water and readily available compound, in the presence of bacteria and an electron donor such as acetate (reaction 1) and used for the reduction of Cr(VI) to Cr (III) (reaction 2) [42,43]. Hydrogen sulphide may be also generated through the reaction of acetate with sulphate ions (reaction 3), if present in wastewaters, and participate again in reaction (2):

$$CH_3COOH + 4S^0 + 4H_2O \rightarrow 2H_2CO_3 + 4H_2S \quad (1)$$

$$2CrO_4^{2-} + 3H_2S + 4H^+ \rightarrow 2Cr(OH)_3 + 3S^0 + 2H_2O \quad (2)$$

$$CH_3COO^- + SO_4{}^{2-} \rightarrow 2HCO_3{}^- + HS^- \quad (3)$$

If a contaminated plume that contains heavy metals and sulphates reacts with organic matter (CH_2O) that contains sulphate-reducing bacteria (SRB), hydrogen sulphide and bicarbonate will be generated (reaction 4). If anaerobic conditions are established then bacterial growth is promoted and the generated hydrogen is used as electron donor by SRBs. In this case, if a divalent ion is present, a sulphide compound will precipitate and acidity will be generated:

$$SO_4{}^{2-} + 2CH_2O \rightarrow H_2S + 2HCO_3{}^- \quad (4)$$

$$Me^{2+} + H_2S \rightarrow MeS\downarrow + 2H^+ \quad (5)$$

The present paper aims to study the removal of Cr (VI) from effluents in sulphur-amended organic PRBs and identify the main mechanisms involved with the use of analytical techniques, namely XRD, SEM-EDS and FTIR.

2. Materials and methodology

2.1. Materials

The organic material used in this study is a commercial fertilizer consisting of goat manure (GOM). It has pH 7 and contains 47% organic matter, 16×10^7 colony forming units g^{-1} and traces of N, P_2O_5, K_2O, Ca, Mg, Fe, Mn, Cu, B, Mo and Zn. Sulphur was used in powder form with 99% purity (Sulphur Mills Limited, India). Limestone, obtained from a local quarry (Finobeton Mining S.A, Chania, Greece), consisted of 97% calcite and 3% dolomite and was ground to −2 mm prior to use, with a Fritsch-Bico Pulverizer (Germany).

Feed solutions were prepared by dissolving potassium dichromate ($K_2Cr_2O_7$) in distilled water, so that the initial Cr(VI) concentration was 10 mg L^{-1}. The feed contained also acetate (0.01 M or 0.1 M) as electron donor and carbon source so that the initial chemical oxygen demand (COD) was either 0.6 or 6 g L^{-1}. The prepared feed represents the quality of plumes existing in the vicinity of disposal areas where chromium-containing wastewaters from leather tanning or electroplating industry are discharged [44–46].

2.2. Experimental set-up

Laboratory experiments were carried out using two plexiglas columns (50 cm length and 5 cm internal diameter) placed in series as shown in Fig. 1. The total dry weight of the bed was 1,300 g, so that the weight of the reactive material in each column was 650 g. In sulphur-amended columns, 180 g of S were added in each column (S/GOM = 0.3 w/w). Two 2.5 cm thick silica sand (average size 1.5 mm) layers were placed at the base and the top of each column in order to ensure optimum flow distribution and prevent loss of fine particles. This configuration was based on previous experience [47] and was used in order to prevent clogging, permeability loss and transfer of fines as well as to increase retention time in the reactive bed and thus improve the efficiency and longevity of the system.

Table 1 shows the experimental set-up. The system containing only GOM was used as control. All experiments were carried out in duplicate. Average results are presented in this study but it is underlined that the difference in system performance was in all cases less than ±5%.

Up-flow was applied in order to eliminate channelling, maintain optimum contact between solution and reactive materials and increase retention time. The solution was pumped in the lower column from 10 L plastic vessels using PROMINENT GAMMA/4 peristaltic pumps at a Darcy velocity of 100 cm d^{-1}.

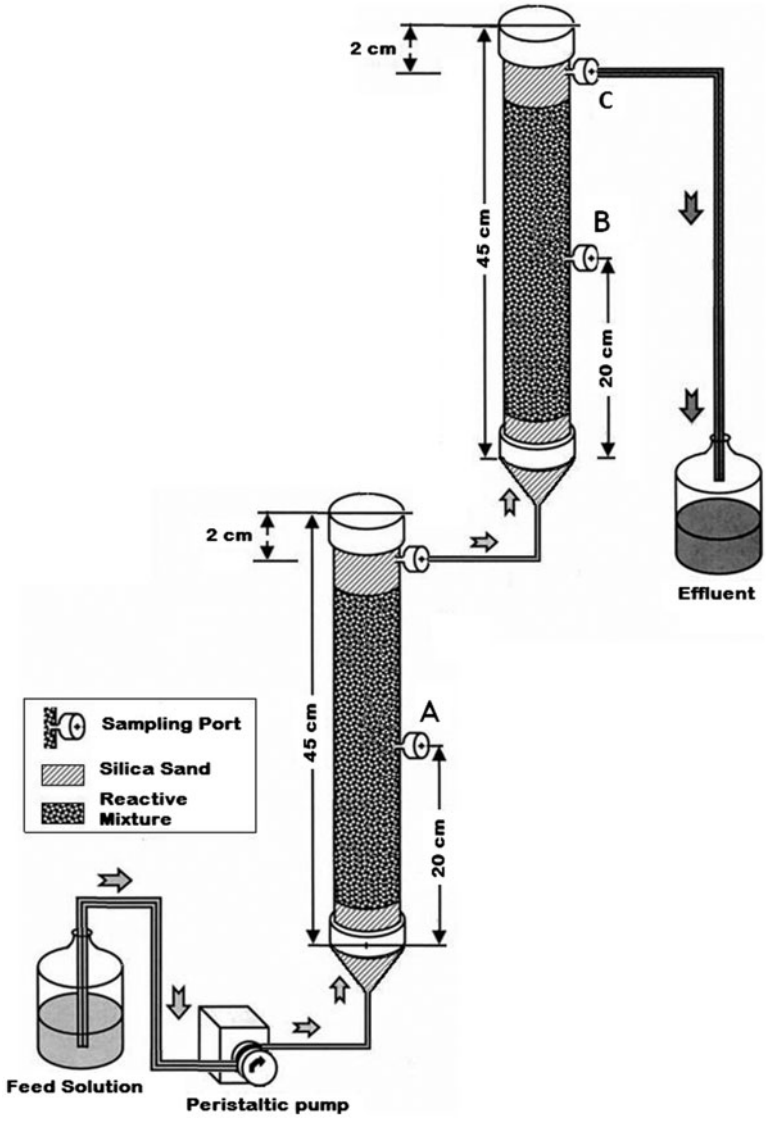

Fig. 1. Laboratory column system [27].

Table 1
Experimental set-up

System	First column	Second column	Feed solution
GOM	Organic material	Organic material	Cr(VI) 10 mg L^{-1}
GOM/L/S/COD6	Organic material + 30% w/w limestone	Organic material + 30% S (w/w)	Cr(VI) 10 mg L^{-1} 0.1 M CH_3COOH
GOM/S/COD6	Organic material + 30% S (w/w)	Organic material + 30% S (w/w)	Cr(VI) 10 mg L^{-1} 0.1 M CH_3COOH
GOM/S/COD0.6	Organic material + 30% S (w/w)	Organic material + 30% S (w/w)	Cr(VI) 10 mg L^{-1} 0.01 M CH_3COOH

Note: GOM: goat manure, L: limestone, S: sulphur, COD6 (COD6 g L^{-1}), and COD0.6 (COD0.6 g L^{-1}).

No problems were noticed pertinent to the stability of the operating solution. The flow rate was maintained at 1.3 ± 0.05 mL min^{-1} so that one pore (total bed) volume (500 mL) was fed every 6.4 h. The total empty bed contact time, defined as the ratio bed length:approach velocity was 20 h. The hydraulic loading rate, calculated by dividing the flow rate with the cross-sectional area, was 0.04 m h^{-1}.

2.3. Chemical and mineralogical analyses

Column effluents were analysed immediately for pH, Eh (the potential of a solution relative to standard hydrogen electrode, SHE) and electrical conductivity using a HANNA pH 211 combined pH/Eh meter and electric conductivity using a HANNA EC 215 EC meter. Solutions were filtered using 0.45 μm acro disk filters prior to analysis. Total Cr concentration was determined using either an AAS (Perkin Elmer Analyst 100 flame atomic absorption spectrophotometer) or a LaMotte Smart3 colorimeter. The difference in measurements did not exceed 3%. Cr(VI), COD, sulphate, phosphate and nitrate concentrations were determined using a LaMotte Smart2 colorimeter. The procedures followed are those described in the instrument's manual. The concentration of Cr(III) was determined by subtracting the Cr(VI) from the total Cr concentration. All analyses were carried out in duplicate.

The actual concentration of hydrogen sulphide in the effluent was determined weekly using a Varian CARY 1E UV–vis spectrophotometer [48]. The theoretical concentration of hydrogen sulphide in the effluent was calculated using the stoichiometry of reaction (1), which indicates that from the oxidation of 1 mg COD 2 mg of hydrogen sulphide are produced. Thus, the free H_2S concentration in the effluent was calculated by subtracting the hydrogen sulphide consumed by reaction (2) from the respective quantity produced from reaction (1). For the determination of the hydrogen sulphide that participates in reaction (1), the net COD consumption (COD_{out}−COD_{in}) was used. The difference between theoretical and measured values was ±5%.

Prior to mineralogical analysis, solid samples of the "exhausted" reactive material were air dried and gently ground using an agate mortar and pestle and then sieved manually. This procedure enabled separation of coarse particles (>140 μm, mostly organic material) from the fines and adequate separation of precipitates. The coarse fraction was hand-ground and sieved two more times in order to adequately remove surface precipitates and obtain a <63 μm fraction that was used for analysis. The material obtained from this procedure was analysed by XRD using a Siemens D500 Diffractometer at 30 kV and 15 mA. SEM analyses were also carried out using a JEOL 6380LV Scanning Electron Microscope equipped with an EDS INCA microanalysis system, under low vacuum, to study the morphology of the formed phases. FTIR analysis was carried out using KBr pellets and a Perkin-Elmer 1000 Spectrometer (USA). For the production of the pellets, each sample was mixed with KBr at a ratio 1:100 w/w.

3. Results and discussion

3.1. Cr(VI) removal

Fig. 2 shows the evolution of effluent pH and Eh vs. time in all systems studied. The effluent pH in the GOM (control) system, where the reactive bed contains only GOM and the feed 10 mg L^{-1} Cr(VI), increases from the initial feed value of 5.6 to almost 8 where it remains until day 45. Then pH drops slowly and reaches 7.2 at the end of the test, after 90 d.

The initial pH of the feed solutions in all other systems is around 3 (pH 3.5 for the system GOM/S/COD0.6 and ~2.9 for the system GOM/S/COD6). The pH of the effluent in the system GOM/L/S/COD6, in which limestone is present in the first column and

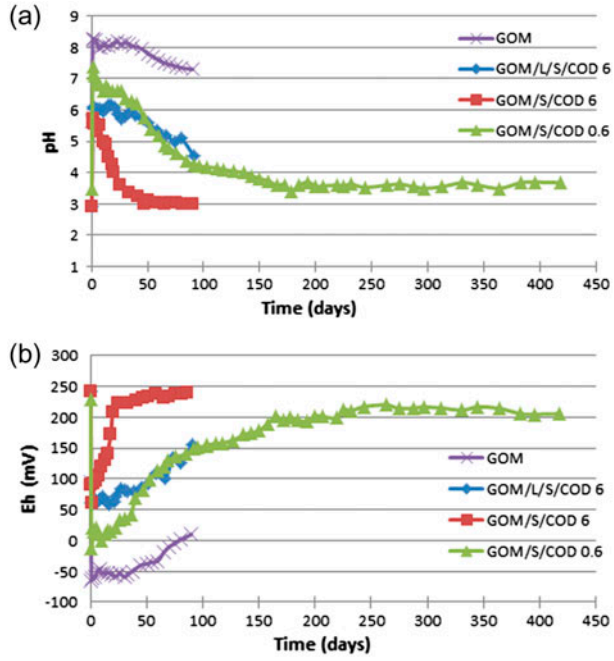

Fig. 2. Evolution of (a) effluent pH and (b) Eh vs. time.

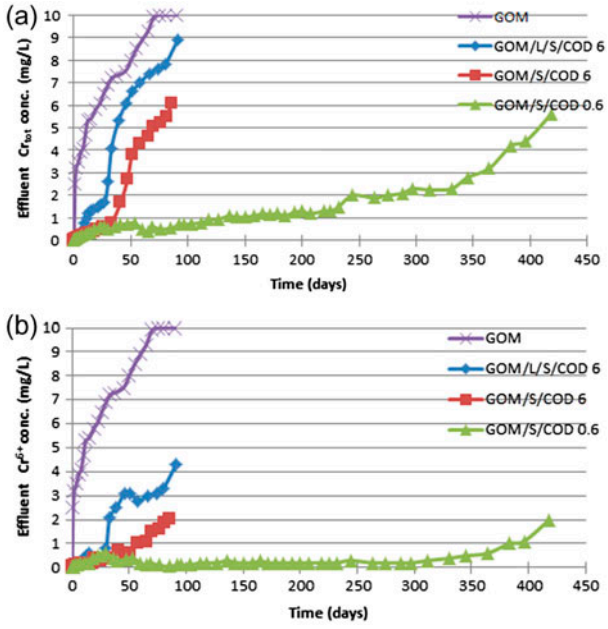

Fig. 3. Evolution of (a) total Cr and (b) Cr(VI) concentration in effluents vs. time.

sulphur in the second one, increases immediately to 6, remains at this level for almost 25 d and then drops gradually and after 90 d reaches the value of 4.6. The pH of the system GOM/S/COD6, in which S is present in both columns, drops much faster and reaches the initial feed value of 3 after 45 d where it is stabilized until the end of the test (90 d). It is thus seen that the presence of limestone in the first column adds alkalinity in the system and improves the buffering capacity of the reactive bed. Finally, the effluent pH of the system GOM/S/COD0.6, in which the feed contains lower COD (0.6 g L^{-1}), increases to 7.8 the first day, drops gradually to 3.5 after 175 d and remains close to this value until the end of the experiment.

Eh values in all systems (Fig. 2(b)) correspond to pH values. It is obvious that net reducing conditions are maintained throughout the experimental period only in the system containing organic material. When the feed contains high COD (6 g L^{-1}), Eh values increase and at the end of the test reach 150 and 250 mV for the systems GOM/L/S/COD6 and GOM/S/COD6, respectively. The Eh in the system with low COD in the feed increases gradually, after 175 d reaches 210 mV and remains at this level until the end of the experiment.

Fig. 3 shows the evolution of total and Cr(VI) concentration in the effluents of all systems studied. When only GOM is used as reactive medium, the system efficiency is limited and total Cr removal is less than 50% just after 10 d. Cr(VI) removal drops gradually and after 70 d practically stops. It is obvious that in this case sorption is the only process involved in chromium removal.

The system GOM/L/S/COD6 that contains limestone in the first column and exhibits higher pH values throughout the experimental period, is also characterized by limited Cr(VI) removal efficiency compared to the system GOM/S/COD6. It is believed that some calcium solubilized from limestone reacts and consumes part of COD according to reaction (6), forming the soluble phase $Ca(CH_3COO)_2$. Thus, the available amount of COD to react with elemental S and produce hydrogen sulphide according to reaction (1), which will in turn induce Cr(VI) removal, is reduced. It is also shown that the total chromium concentration in the effluent increases more sharply when the pH values drop below 6 (Fig. 3(a)). In this system, almost half of the chromium present in the effluent is in the form of Cr(III). The system GOM/S/COD6 performs very well the first 35 d and the Cr concentration in the effluent is lower than 1 mg L^{-1}. Then, the reactivity of the system drops gradually and after 85 d only 40% of chromium is retained (total Cr concentration in the effluent 6 mg L^{-1}).

$$2CH_3COOH + CaCO_3 \rightarrow Ca(CH_3COO)_2 + 4H_2CO_3 \quad (6)$$

The system GOM/S/COD0.6 shows much better Cr (VI) removal efficiency. Total effluent chromium concentration does not exceed 1 mg L^{-1} the first 150 d. Then it starts to increase slowly, after 250 d reaches 2 mg L^{-1}, after 370 d exceeds 3 mg L^{-1} and after 420 d reaches 5.8 mg L^{-1}. The concentration of Cr(VI) remains below 0.3 mg L^{-1} for the first 300 d and then increases slowly and after 420 d reaches 2 mg L^{-1}. So, most of the Cr present in the effluent during the entire experimental period is in the form of Cr(III).

The experimental results indicate that Cr(VI) is reduced according to reaction (2) using the hydrogen sulphide produced by reaction (1), when the COD of the feed reacts with the S present in the reactive bed. It is believed that in the reactive zone, the following half reactions (7) and (8) may take place and result in the reduction of Cr(VI) as Cr(III):

$$Cr_2O_7^{2-}\ (aq) + 14H^+\ (aq) + 6e^-\ \rightarrow 2Cr^{3+}(aq) + 7H_2O \quad E^\circ = +1.33\ V \tag{7}$$

$$H_2S + 4H_2O \rightarrow SO_4^{2-} + 10H^+ + 8e^- \quad E^\circ = +0.221V \tag{8}$$

If reactions (7) and (8) are added, the overall reaction (9) derives:

$$Cr_2O_7^{2-} + H_2S + 4H^+ \rightarrow 2Cr^{3+} + SO_4^{2-} + 3H_2O \quad E^\circ = +1.551V \tag{9}$$

Fig. 4 shows the evolution of effluent COD while Fig. 5 the calculated free H_2S concentration vs. time in all systems studied.

It is shown in Fig. 4 that in all systems, only part of COD reacts with sulphur. When the initial COD is 6 g L^{-1}, an initial drop in its effluent concentration is shown for the first 15 d and then for the remaining period the concentration varies between 4 and 4.5 g L^{-1}. The final

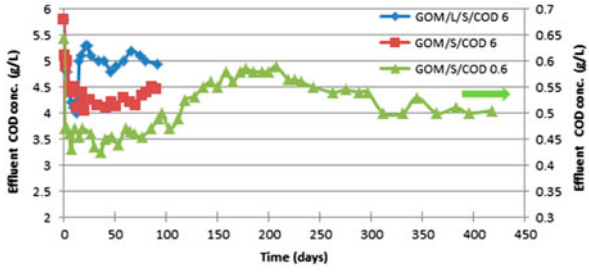

Fig. 4. Evolution of effluent COD vs. time.

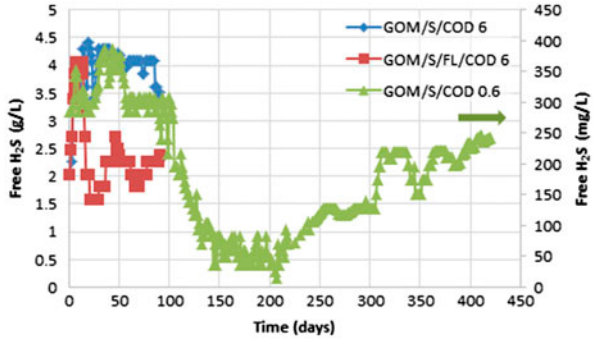

Fig. 5. Evolution of effluent free H_2S concentration vs. time.

effluent COD concentration is slightly higher in the system GOM/L/S/COD6 (approx. 5 g L^{-1}) compared to the system GOM/S/COD6 (4–4.5 g L^1). Thus in the GOM/L/S/COD6 system COD oxidation is around 15% for most of the experimental period, while in the GOM/S/COD6 increases to 25–30%. In the most efficient system GOM/S/COD0.6, the effluent COD concentration is quite stable for the first 100 d (0.45 g L^{-1}) and then increases and reaches 0.55–0.6 g L^{-1} after 160 d. Then COD concentration drops gradually and in the last 100 d is approx. 0.5 g L^{-1}. It is mentioned that the effluent COD concentration in the GOM system does not exceed 40 mg L^{-1}. Calculations based on reactions given earlier prove that even if 10% or less of the incoming COD reacts with sulphur, sufficient H_2S is generated to reduce Cr(VI) as Cr(III).

An issue that needs further elucidation though is why the system with less incoming COD (GOM/S/COD0.6) behaves better that the system with 10 times more incoming COD (GOM/S/COD6). There are very little studies on this issue which indeed confirm the results of the present study. Gyure et al. [49] mention that high concentrations (5 mM) of organic acids inhibit sulphate reduction at pH 3.8, whereas stimulation was observed at concentrations of 0.1 mM. Koschorreck et al. [50] mention that acetate concentration above 15 mM (900 mg L^{-1}) inhibits sulphate reduction, while if the acetate concentration is above 94 mM (5,640 mg L^{-1}) the inhibition is nearly complete. In our study, the incoming COD concentration was 6,000 mg L^{-1} for the system GOM/S/COD6 and 600 mg L^{-1} for the system GOM/S/COD0.6. Furthermore, Muthumbi et al. [51] mention that sodium in high concentrations may also inhibit sulphate reduction, but in our system practically no Na exists.

It is shown from Fig. 5 that the concentration of free H_2S in the effluent in the system with the optimum performance (GOM/S/COD0.6) drops after day 50 and reaches values varying between 50 and 100 mg L^{-1} after

120–220 d. Then it increases gradually and at the end of the test, after 420 d, reaches 225 mg L^{-1}. This is the period that the system shows the optimum efficiency and thus most of the H_2S produced is consumed. These data are confirmed by visual observations showing that bubble formation after day 200 is limited. Other researchers indicated similar residual-dissolved sulphide concentrations during effluent clean-up studies for the removal of Pb, Zn and Fe [52].

Figs. 6 and 7 show the evolution of effluent SO_4 and COD/SO_4 vs. time in all enriched with acetic acid systems. It is shown in Fig. 6 that the system with the best performance, GOM/S/COD0.6, exhibits at the end of the run limited SO_4 concentrations, which are below the threshold for discharging effluents. On the other hand, in the same system, increased COD/SO_4 ratios are observed which exhibit two plateaus, one at around 300 between day 130 and day 230 and the second at around 500 during the last 150 d (Fig. 7).

Experimental data are in agreement with other studies investigating Cr removal from effluents and wastewaters. It has been reported that increased COD/SO_4 ratios in wastewaters improve hydrogen sulphide production that induces heavy metal precipitation [53]. Other researchers suggest that COD/SO_4 ratios varying between 1.5 and 2.25 could attain high hydrogen sulphide production when acetate or lactate was used as carbon and electron source [54]. Jeong et al. [55] mention that the rate of hydrogen sulphide production in anaerobic digestion studies using waste activated sludge decreases when the COD concentration in the feed is high and thus the COD/SO_4 ratio also becomes high. The same authors mention that this aqueous sulphide system is complicated due to the dissociation equilibrium of soluble sulphide, which has the equilibrium between gaseous and aqueous hydrogen sulphide. The equilibrium between these two phases is governed by the solubility of unionized H_2S species which is defined by the Henry's law.

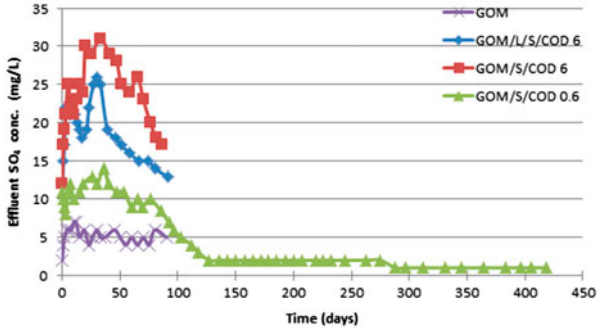

Fig. 6. Evolution of effluent SO_4 vs. time.

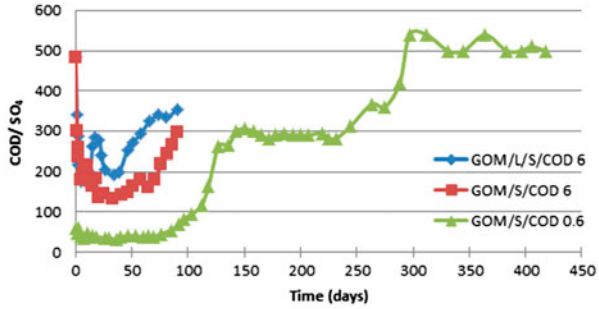

Fig. 7. Evolution of effluent COD/SO_4 vs. time.

3.2. Mineralogical studies

The XRD pattern of the <63 μm fraction of precipitates formed in the GOM/S/COD6 system is shown in Fig. 8. XRD analyses show that apart from sulphur, several new low-intensity peaks appear indicating the formation of $Cr(OH)_3$ as a result of the reduction of Cr(VI) to Cr(III). The XRD pattern has a high background noise due to the presence of organic material in the sample and the corresponding peaks of Cr-precipitated phases have been slightly shifted.

Previous studies mention that the reduction of Cr(VI) is more complex than the direct production of insoluble Cr(III) phases [56,57]. In this study, the reduction of Cr(VI) to Cr(III) was also visually noticed through the disappearance of the yellow colour of the chromate-containing solution and the formation of a green/violet Cr(III) precipitate.

SEM and EDS analyses were also carried out to examine the surface morphology of the exhausted material, identify newly formed phases and their elemental composition and in turn to elucidate the main Cr removal mechanisms involved. Fig. 9 shows a SEM

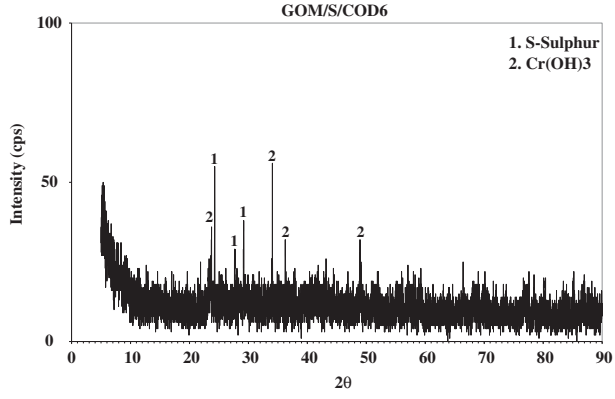

Fig. 8. XRD pattern of precipitates in the "exhausted" GOM/S/COD6 system.

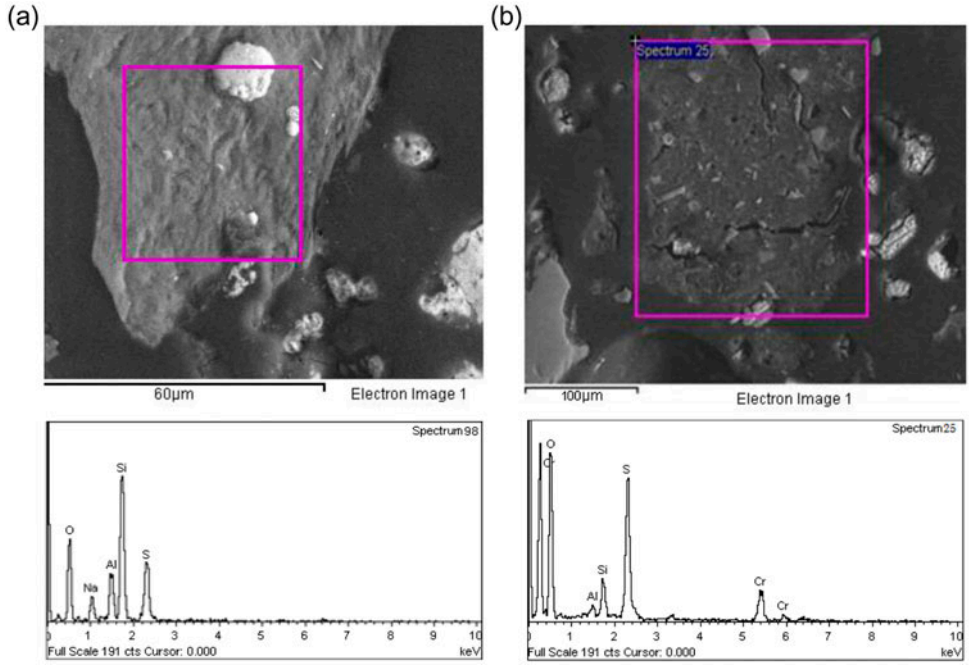

Fig. 9. (a) SEM-BSI and EDS spectra of "raw GOM/S/COD6 mixture", scale 60 µm. (b) SEM-BSI and EDS spectra of "exhausted GOM/S/COD6 mixture", scale 100 µm.

backscattered image of the GOM/S/COD6 reactive mixture (a) prior to and (b) after column runs.

Chromium-loaded samples of the "exhausted" GOM/S/COD6 mixture show different surface morphology compared to the unloaded samples of the same mixture. The matrix of the raw GOM/S/COD6 mixture (prior to column tests) exhibited an inflated shape with a distinct external layer on the outer edge surface, which became coated, shrunk and even cracked after feeding of several loads of chromium-containing leachates in the system. This structural change of the reactive matrix indicates that the primary chromium sorption sites are located on the inner surface instead of the outer edge sites. The corresponding EDS spectra before and after chromium uptake, provide further evidence of the strong bond of Cr(III) ions and negatively charged chemical groups on GOM/S/COD6 system as a result of Cr(VI) reduction. Signals of significant chromium content (up to ~6% wt.) were detected on the exhausted inner matrix of the reactive mixture. However, it is not fully evident that the chromium content on the exhausted GOM/S/COD6 mixture is only due to precipitates of adsorbed Cr(III) and/or surface coatings of non-reduced Cr(VI). It is believed that the overall reaction for Cr(VI) reduction mainly follows in general the stoichiometry represented by reaction (9). As a result of this reaction, the concentration of SO_4 in the effluent of the GOM/S/COD6 system increased after 40 d to 31 mg L^{-1} and then gradually decreased.

Fig. 10 shows the FTIR spectra of the "exhausted" GOM/S/COD0.6 reactive mixture, while the FTIR spectra band assignments are presented in Table 2.

The broad peak seen at around 3,440 cm^{-1} indicates the presence of hydroxyl group (−OH) stretching on the surface of the organic material. All other bands are due to the presence of organic matter constituents, such as short aliphatic chains, polysaccharides and alcohols. The peaks at 2,855 and 2,920 cm^{-1} are

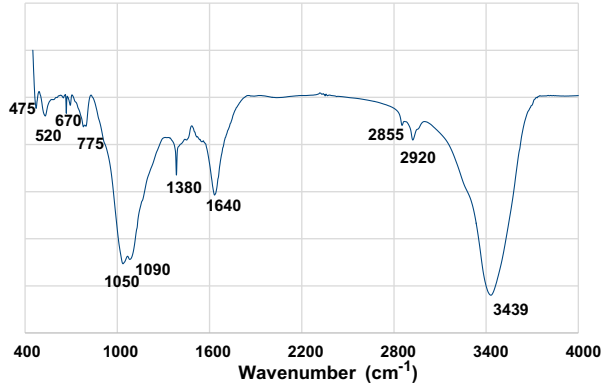

Fig. 10. FTIR spectra of the exhausted GOM/S/COD0.6 reactive mixture.

Table 2
FTIR spectra band assignments

Band number (cm^{-1})	Assignment
3,439	Hydroxyl group (−OH) stretching
2,855, 2,920	Aliphatic C–H deforming vibration
1,640	Aromatic C=O ring or C=C stretching, N–H bending
1,380	δ(C=H) vibration in alkanes and alkyl groups
1,050, 1,090	C–C−O or C–O−C asymmetric stretching or C–O stretching
475–775	C–H wagging vibrations

ascribed to aliphatic C–H deforming vibration [58,59]. The sharp peak at around 1,640 cm^{-1} is due to the presence of aromatic C=O ring or C=C stretching or due to N–H bending of amide.

The band at 1,380 cm^{-1} is attributed to δ(C=H) vibration in alkanes and alkyl groups [60]. The broad bands at 1,050 and 1,090 cm^{-1} are characteristic of a C–C−O or C–O−C asymmetric stretching or due to C–O stretching of polysaccharide. All these functional groups may be preferable for binding Cr(VI) ions on the organic material surface [61,62]. In the region 475–775 cm^{-1}, aromatic and heteroaromatic compounds are confirmed by C–H wagging vibrations.

4. Conclusions

This novel study proves that composite PRBs, containing organic material and elemental sulphur, can be used for the effective clean-up of contaminated leachates containing 10 mg L^{-1} Cr(VI) and 0.6 M COD. The average chromium removal efficiency for the GOM/S/COD0.6 system over a period of 270 d was 7.92 mg g^{-1}.

The major effects of COD/SO_4 ratio and organic material load on Cr(VI) removal rates were mainly associated with sorption, hydrogen sulphide generation and presence of a carbon source. Mineralogical studies of the exhausted reactive mixture using XRD, SEM/EDS and FTIR confirm the formation of new precipitated phases, such as $Cr(OH)_3$.

Although Cr(VI) was effectively removed in the laboratory, using reactive beds containing sulphur-amended organic material, additional research is required prior to potential applications of such PRBs in the field to predict their reactivity in the co-presence of other inorganic and organic contaminants as well as their hydraulic performance, by considering effects such as bioclogging and biofouling.

On the other hand, it has to be taken into account that in field applications the hydrogeological conditions that prevail may result in a substantial increase in the effective Cr(VI) removal rate. It is known that the average groundwater flow rate in PRBs operating in the field is much lower (0.3 m d^{-1}) than the flow rate (1 m d^{-1}) considered in the present study, thus higher residence times are anticipated.

References

[1] L. Shakir, S. Ejaz, M. Ashraf, N.A. Qureshi, A.A. Anjum, I. Iltaf, A. Javeed, Ecotoxicological risks associated with tannery effluent wastewater, Environ. Toxicol. Pharmacol. 34 (2012) 180–191.
[2] S. Martinez-Delgadillo, H. Mollinedo-Ponce, V. Mendoza-Escamilla, C. Gutiérrez-Torres, J. Jiménez-Bernal, C. Barrera-Diaz, Performance evaluation of an electrochemical reactor used to reduce Cr(VI) from aqueous media applying CFD simulations, J. Clean. Prod. 34 (2012) 120–124.
[3] A.G. Tekerlekopoulou, M. Tsiflikiotou, L. Akritidou, A. Viennas, G. Tsiamis, S. Pavlou, K. Bourtzis, D.V. Vayenas, Modelling of biological Cr(VI) removal in draw-fill reactors using microorganisms in suspended and attached growth systems, Water Res. 42 (2013) 623–636.
[4] European Commission, Council Directive 98/83/EC on the Quality of Water Intended for Human Consumption, Official Journal of the European Communities, L330/32-54, November 3, 1998.
[5] M.C. Brum, J.L. Capitaneo, J.F. Oliveira, Removal of hexavalent chromium from water by adsorption onto surfactant modified montmorillonite, Miner. Eng. 23 (2010) 270–272.
[6] C.E. Barrera-Díaz, V. Lugo-Lugo, B. Bilyeu, A review of chemical, electrochemical and biological methods for aqueous Cr(VI) reduction, J. Hazard. Mater. 223–224 (2012) 1–12.
[7] C. Noubactep, K.B.D. Btatkeu, J.B. Tchatchueng, Impact of MnO_2 on the efficiency of metallic iron for the removal of dissolved Cr VI, Cu II, Mo VI, Sb V, U VI and Zn II, Chem. Eng. J. 178 (2011) 78–84.
[8] Q. Wang, N. Chen, Y. Yu, C. Feng, Q. Ning, W. Hu, Chromium(VI) removal from aqueous solution using a new synthesized adsorbent, Desalin. Water Treat. (2014), doi: 10.1080/19443994.2014.992968.
[9] J. Buerge, S.J. Hug, Kinetics and pH dependence of chromium (VI) reduction by iron(II), Environ. Sci. Technol. 31 (1997) 1426–1432.
[10] M. Gheju, I. Balcu, Removal of chromium from Cr(VI) polluted wastewaters by reduction with scrap iron and subsequent precipitation of resulted cations, J. Hazard. Mater. 196 (2011) 131–138.
[11] N. Melitas, O. Chuffe-Moscoso, J. Farrell, Kinetics of chromium removal from contaminated water by zero valent iron media: Corrosion inhibition and passive oxide effects, Environ. Sci. Technol. 35 (2001) 3948–3953.
[12] Q. Wang, H. Qian, Y. Yang, Z. Zhan, C. Naman, X. Xu, Reduction of hexavalent chromium by carboxymethyl

cellulose-stabilized zero-valent iron nanoparticles, J. Contam. Hydrol. 114 (2010) 35–42.
[13] C. Mystrioti, A. Xenidis, N. Papassiopi, Reduction of hexavalent chromium with polyphenol-coated nano zero-valent iron: Column studies, Desalin. Water Treat. (2014), doi: 10.1080/19443994.2014.941298.
[14] J. Chung, R. Nerenberg, B.E. Rittmann, Bio-reduction of soluble chromate using a hydrogen-based membrane biofilm reactor, Water Res. 40 (2006) 1634–1642.
[15] N.M. Dogan, C. Kantar, S. Gulcan, C.J. Dodge, B.C. Yilmaz, M.A. Mazmanci, Chromium (VI) bioremoval by *Pseudomonas* bacteria: Role of microbial exudates for natural attenuation and biotreatment of Cr(VI) contamination, Environ. Sci. Technol. 45 (2011) 2278–2285.
[16] R. Elengovan, L. Philip, Performance evaluation of various bioreactors for the removal of Cr(VI) and organic matter from industrial effluent, Biochem. Eng. J. 44 (2009) 174–186.
[17] R. Kumar, N.R. Bishnoi, Garima, K. Bishnoi, Biosorption of chromium(VI) from aqueous solution and electroplating wastewater using fungal biomass, Chem. Eng. J. 135 (2008) 202–208.
[18] S.E. Lee, J.U. Lee, H.T. Chon, J.S. Lee, Microbiological reduction of hexavalent chromium by indigenous chromium-resistant bacteria in sand column experiments, Environ. Geochem. Health 30 (2008) 141–145.
[19] F. Pagnanelli, C. Cruz Viggi, A. Cibati, D. Uccelletti, L. Toro, C. Palleschi, Biotreatment of Cr(VI) contaminated waters by sulphate reducing bacteria fed with ethanol, J. Hazard. Mater. 199–200 (2012) 186–192.
[20] A.S. Stasinakis, N.S. Thomaidis, D. Mamais, T.D. Lekkas, Investigation of Cr(VI) reduction in continuous-flow activated sludge systems, Chemosphere 57 (2004) 1069–1077.
[21] E. Vaiopoulu, P. Gikas, Effects of chromium on activated sludge and on the performance of wastewater treatment plants: A review, Water Res. 46 (2012) 549–570.
[22] K. Katsaveli, D. Vayenas, G. Tsiamis, K. Bourtzis, Bacterial diversity in Cr(VI) and Cr(III)-contaminated industrial wastewaters, Extremophiles 16 (2012) 285–296.
[23] C.S.C. Calheiros, P.V.B. Quitério, G. Silva, L.F.C. Crispim, H. Brix, S.C. Moura, P.M.L. Castro, Use of constructed wetland systems with *Arundo* and *Sarcocornia* for polishing high salinity tannery wastewater, J. Environ. Manage. 95 (2012) 66–71.
[24] A.N. Módenes, F.R. Espinoza-Quiñones, F.H. Borba, D.R. Manenti, Performance evaluation of an integrated photo-Fenton—Electrocoagulation process applied to pollutant removal from tannery effluent in batch system, Chem. Eng. J. 197 (2012) 1–9.
[25] S.A. Cavaco, S. Fernandes, C.M. Augusto, M.J. Quina, L.M. Gando-Ferreira, Evaluation of chelating ion-exchange resins for separating Cr(III) from industrial effluents, J. Hazard. Mater. 169 (2009) 516–523.
[26] E. Piedra, J.R. Álvarez, S. Luque, Hexavalent chromium removal from chromium plating rinsing water with membrane technology, Desalin. Water Treat. 53 (2015) 1431–1439.
[27] G. Bartzas, K. Komnitsas, I. Paspaliaris, Laboratory evaluation of Fe0 barriers to treat acidic leachates, Miner. Eng. 19 (2006) 505–514.
[28] D.H. Phillips, T.V. Nooten, L. Bastiaens, M.I. Russell, K. Dickson, S. Plant, J.M.E. Ahad, T. Newton, T. Elliot, R.M. Kalin, Ten year performance evaluation of a field-scale zero-valent iron permeable reactive barrier installed to remediate trichloroethene contaminated groundwater, Environ. Sci. Technol. 44 (2010) 3861–3869.
[29] R.T. Wilkin, C. Su, R.G. Ford, C.J. Paul, Chromium-removal processes during groundwater remediation by a zerovalent iron permeable reactive barrier, Environ. Sci. Technol. 39 (2005) 4599–4605.
[30] K. Komnitsas, G. Bartzas, I. Paspaliaris, Efficiency of limestone and red mud barriers: Laboratory column studies, Miner. Eng. 17 (2004) 183–194.
[31] J. Yang, L. Cao, R. Guo, J. Jia, Permeable reactive barrier of surface hydrophobic granular activated carbon coupled with elemental iron for the removal of 2,4-dichlorophenol in water, J. Hazard. Mater. 184 (2010) 782–787.
[32] A.D. Henderson, A.H. Demond, Permeability of iron sulfide (FeS)-based materials for groundwater remediation, Water Res. 47 (2013) 1267–1276.
[33] M.R. Boni, S. Sbaffoni, The potential of compost-based biobarriers for Cr(VI) removal from contaminated groundwater: Column test, J. Hazard. Mater. 166 (2008) 1087–1110.
[34] V.K. Gupta, A. Rastogi, A. Nayak, Adsorption studies on the removal of hexavalent chromium from aqueous solution using a low cost fertilizer industry waste material, J. Colloid Interface Sci. 342 (2010) 135–141.
[35] O. Gibert, J. De Pablo, J.-L. Cortina, C. Ayora, In situ removal of arsenic from groundwater by using permeable reactive barriers of organic matter/limestone/zero-valent iron mixtures, Environ. Geochem. Health 32 (2010) 373–378.
[36] N. Moraci, P.S. Calabrò, Heavy metals removal and hydraulic performance in zero-valent iron/pumice permeable reactive barriers, J. Environ. Manage. 91 (2010) 2336–2341.
[37] F. Pagnanelli, C.C. Viggi, S. Mainelli, L. Toro, Assessment of solid reactive mixtures for the development of biological permeable reactive barriers, J. Hazard. Mater. 170 (2009) 998–1005.
[38] G. Bartzas, K. Komnitsas, Solid phase studies and geochemical modelling of low-cost permeable reactive barriers, J. Hazard. Mater. 183 (2010) 301–308.
[39] C. Noubactep, S. Caré, Designing laboratory metallic iron columns for better result comparability, J. Hazard. Mater. 189 (2001) 809–813.
[40] I.S. Chang, B. Kim, Effect of sulfate reduction activity on biological treatment of hexavalent chromium [Cr (VI)] contaminated electroplating wastewater under sulfate-rich condition, Chemosphere 67 (2007) 218–226.
[41] E. Sahinkaya, A. Kilic, M. Altun, K. Komnitsas, P.N.L. Lens, Hexavalent chromium reduction in a sulfur reducing packed-bed bioreactor, J. Hazard. Mater. 219–220 (2012) 253–259.
[42] C. Kim, Q. Zhou, B. Deng, E.C. Thornton, H. Xu, Chromium(VI) reduction by hydrogen sulfide in aqueous media: Stoichiometry and kinetics, Environ. Sci. Technol. 35 (2001) 2219–2225.
[43] E. Sahinkaya, M. Altun, S. Bektas, K. Komnitsas, Bioreduction of Cr(VI) from acidic waste waters in a sulfidogenic ABR, Miner. Eng. 32 (2012) 38–44.
[44] UNIDO (2000), United Nations Industrial Development Organization, Pollutants in Tannery Effluents,

US/RAS/92/120, by: M. Bosnic, J. Buljan, R.P. Daniels. Available from: <http://www.unido.org/fileadmin/user_media/Publications/Pub_free/Pollutants_in_tannery_effluents.pdf> (accessed on Dec 15, 2014).
[45] G.M. Ayoub, A. Hamzeh, L. Semerjian, Post treatment of tannery wastewater using lime/bittern coagulation and activated carbon adsorption, Desalination 273 (2011) 359–365.
[46] S. Sharma, A. Adholeya, Detoxification and accumulation of chromium from tannery effluent and spent chrome effluent by *Paecilomyces lilacinus* fungi, Int. Biodeterior. Biodegrad. 65 (2011) 309–317.
[47] K. Komnitsas, G. Bazdanis, E. Sahinkaya, G. Bartzas, D. Zaharaki, Removal of heavy metals from leachates using permeable reactive barriers filled with reactive organic/inorganic mixtures, Desalin. Water Treat. 51 (2013) 3052–3059.
[48] R. Cord-Ruwisch, A quick method for the determinatioon of dissolved and precipitated sulfides in cultures of sulfate-reducing bacteria, J. Microbiol. Methods 4 (1985) 33–36.
[49] R.A. Gyure, A. Konopka, A. Brooks, W. Doemel, Microbial sulfate reduction in acidic (pH 3) strip-mine lakies, FEMS Microbiol. Ecol. 73 (2009) 193–201.
[50] M. Koschorreck, T. Kunze, G. Luther, E. Bozau, K. Wendt-Potthoff, Accumulation and inhibitory effects of acetate in a sulphate reducing in situ reactor for the treatment of an acidic pit lake, in: A.P. Jarvis, B.A. Dudgeon, P.L. Younger (Eds.), Mine Water 2004—Process, Policy and Progress, IMWA Symposium, Newcastle Upon Tyne, International Mine Water Association (IMWA), UK, September 19–23, 2004, pp. 101–109.
[51] W. Muthumbi, N. Boon, R. Boterdaele, I. De Vreese, E.M. Top, W. Verstraete, Microbial sulphate reduction of the bacterial communities in the reactor at different salinity levels, Appl. Microbiol. Biotechnol. 55 (2001) 787–793.
[52] A.H. Kaksonen, P.D. Franzmann, J.A. Puhakka, Performance and ethanol oxidation kinetics of a sulfate-reducing fluidized-bed reactor treating acidic metal-containing wastewater, Biodegradation 14 (2003) 207–217.
[53] A. Velasco, M. Ramírez, T. Volke-Sepúlveda, A. González-Sánchez, S. Revah, Evaluation of feed COD/sulfate ratio as a control criterion for the biological hydrogen sulfide production and lead precipitation, J. Hazard. Mater. 151 (2008) 407–413.
[54] M.A. El Bayoumy, J.K. Bewtra, H.I. Ali, N. Biswas, Sulfide production by sulfate reducing bacteria with lactate as feed in an upflow anaerobic fixed film reactor, Water Air Soil Pollut. 112 (1999) 67–84.
[55] T.-Y. Jeong, G.-C. Cha, Y.-C. Seo, C. Jeon, S.S. Choi, Effect of COD/sulfate ratios on batch anaerobic digestion using waste activated sludge, J. Ind. Eng. Chem. 14 (2008) 693–697.
[56] G.J. Puzon, A.G. Roberts, D.M. Kramer, L. Xun, Formation of soluble organo-chromium(III) complexes after chromate reduction in the presence of cellular organics, Environ. Sci. Technol. 39 (2005) 2811–2817.
[57] V.O. Arief, K. Tilestari, J. Sunarso, N. Indraswati, S. Ismadji, Recent progress on biosorption of heavy metals from liquids using low cost biosorbents: Characterization, biosorption parameters and mechanism studies, CLEAN—Soil Air Water 36 (2008) 937–962.
[58] S. Yaman, Pyrolysis of biomass to produce fuels and chemical feedstocks, Energy Convers. Manage. 45 (2004) 651–671.
[59] Z. Liu, A. Quek, S.K. Hoekman, R. Balasubramanian, Production of solid biochar fuel from waste biomass by hydrothermal carbonization, Fuel 103 (2013) 943–949.
[60] A. Caglar, A. Demirbas, Conversion of cotton cocoon shell to liquid products by pyrolysis, Energy Convers. Manage. 41 (2000) 1749–1756.
[61] N. Ahalya, R.D. Kanamadi, T.V. Ramachandra, Biosorption of chromium (VI) from aqueous solutions by the husk of Bengal gram (*Cicer arientinum*), Electron. J. Biotechnol. 8 (2005) 258–264.
[62] R. Singh, A. Kumar, A. Kirrolia, R. Kumar, N. Yadav, N.R. Bishnoi, R.K. Lohchab, Removal of sulphate, COD and Cr(VI) in simulated and real wastewater by sulphate reducing bacteria enrichment in small bioreactor and FTIR study, Bioresour. Technol. 102 (2011) 677–682.